J Comput Aided Mol Des (2010) 24:879–886
DOI 10.1007/s10822-010-9380-2

# Influence of metal cofactors and water on the catalytic mechanism of creatininase-creatinine in aqueous solution from molecular dynamics simulation and quantum study

**Vannajan Sanghiran Lee · Kanchanok Kodchakorn · Jitrayut Jitonnom · Piyarat Nimmanpipug · Prachya Kongtawelert · Bhusana Premanode**

Received: 3 January 2010 / Accepted: 12 August 2010 / Published online: 28 August 2010


**Abstract** The reaction mechanism of creatinine-creatininase binding to form creatine as a final product has been investigated by using a combined ab initio quantum mechanical/molecular mechanical approach and classical molecular dynamics (MD) simulations. In MD simulations, an X-ray crystal structure of the creatininase/creatinine was modified for creatininase/creatinine complexes and the MD simulations were run for free creatininase and creatinine in water. MD results reveal that two X-ray water molecules can be retained in the active site as catalytic water. The binding free energy from Molecular Mechanics Poisson-Boltzmann Surface Area calculation predicted the strong binding of creatinine with $Zn^{2+}$, Asp45 and Glu183. Two step mechanisms via $Mn^{2+}/Zn^{2+}$ (as in X-ray structure) and $Zn^{2+}/Zn^{2+}$ were proposed for water adding step and ring opening step with two catalytic waters. The pathway using synchronous transit methods with local density approximations with PWC functional for the fragment in the active region were obtained. Preferable pathway $Zn^{2+}/Zn^{2+}$ was observed due to lower activation energy in water adding step. The calculated energy in the second step for both systems were comparable with the barrier of 26.03 and 24.44 kcal/mol for $Mn^{2+}/Zn^{2+}$ and $Zn^{2+}/Zn^{2+}$, respectively.

**Keywords** Creatininase-creatinine · Catalytic mechanism · Molecular dynamics simulation · Quantum mechanics

## Introduction

Dialysis and kidney transplantation are currently available and essential treatments for patients with kidney-related diseases to prolong their lives. Determination of urea concentration in effluent dialysate is widely used as a marker for monitoring urea clearance and other toxic molecules during dialysis. Conventional methods, for instance, spectrophotometric technique, although being considered acceptably accurate, are not practical for real-time monitoring analyzers. The diagnostic analysis of creatinine levels in human blood becomes a clinically important index of renal glomerular filtration rate [1, 2] for real-time monitoring. During kidney disfunctioning or muscle disorder, the creatinine concentration in serum may rise to extremely high level above the normal ranges of serum creatinine and urine creatinine, which typically fall in the range of 35–140 μM and 71–265 μmol · $day^{-1}$ $kg^{-1}$, respectively [3, 4]. The development of potentiometric biosensors with an enzyme-based field effect transistor (ENFETTs) and ion sensitive field effect transistors were applied for urea determination based on the immobilization of urease or creatinase [5]. However, non-linear

**Electronic supplementary material** The online version of this article (doi:10.1007/s10822-010-9380-2) contains supplementary material, which is available to authorized users.

V. S. Lee (✉) · J. Jitonnom · P. Nimmanpipug
Computational Simulation and Modeling Laboratory (CSML), Department of Chemistry and Center for Innovation in Chemistry, Thailand Center of Excellence in Physics (ThEP), Faculty of Science, Chiang Mai University, Chiang Mai 50200, Thailand
e-mail: vannajan@gmail.com

K. Kodchakorn · P. Kongtawelert
Thailand Excellence Center for Tissue Engineering and Stem Cells, Department of Biochemistry, Faculty of Medicine, Chiang Mai University, Chiang Mai 50200, Thailand

B. Premanode (✉)
Institute of Biomedical Engineering, Imperial College, London, UK
e-mail: bhusana@gmail.com

responses and interferences due to ammonia and other ionic substances are undesirable effect and cause the disadvantage from the device. Recently, low power biosensor for real time monitoring of creatinine and urea in peritoneal dialysis demonstrate a linear relationship of urea and creatinine at the range of 0–200 and 0–20 mM, respectively [6]. The sensitivity and stability of the biosensor strongly depend on enzymatic activity and stability. Creatininase is a hydrolytic enzyme that is a member of the urease-related amidohydrolase superfamily. It is a creatinine-metabolizing enzyme and catalyzes the reversible conversion of creatinine (CRE) to creatine, which is a final product of creatine metabolism in mammals.

In order to understand structure–function relationships of the creatininase, an X-ray crystallographic structural analysis of creatininase has illustrated two water molecules and binuclear metal center in the active sites, $Zn^{2+}$ and $Mn^{2+}$, which are potentially essential for the catalytic mechanism of the enzyme. $Zn^{2+}$ has a tetrahedral geometry in its shape and bound to three enzyme amino acids, namely His36, Asp45, and Glu183. Whereas, $Mn^{2+}$ has a square-pyramidal geometry bound to Glu34, Asp45, and His120. The absorption analysis depicts the presence of two zinc ions per subunit in native creatininase, indicating that a higher temperature factor of Zn from native creatininase truly reflects flexibility of Zn. These findings unravel why one of Zn ions was easily replaced, as observed in the crystal structure with $Mn^{2+}$ by the addition of $MnCl_2$ into the culture medium [7]. The possible mechanism has been proposed [7–9] as a two-step catalytic mechanism by Yoshimoto et al. in Fig. 1. However, such mechanism has not been thoroughly proved theoretically on the role of water and the different types of transition metals on the binding between creatininase-creatinine.

In this study, we investigated the previously proposed two-step catalytic mechanism by using quantum mechanical (QM) approach and classical molecular dynamics (MD) simulations. Firstly, the common mechanism involving in the water-adding step when one water molecule acts as the interference of the biological transition metals of $Zn^{2+}$ and $Mn^{2+}$ is determined. The possible nucleophile attacking through the coordination with metals and subsequently followed by the ring-opening step when water acts as the catalytic acid is next studied. The role of water and different metal cofactors on the catalytic mechanism of creatininase-creatinine in aqueous solution from molecular dynamics simulations is then discussed.

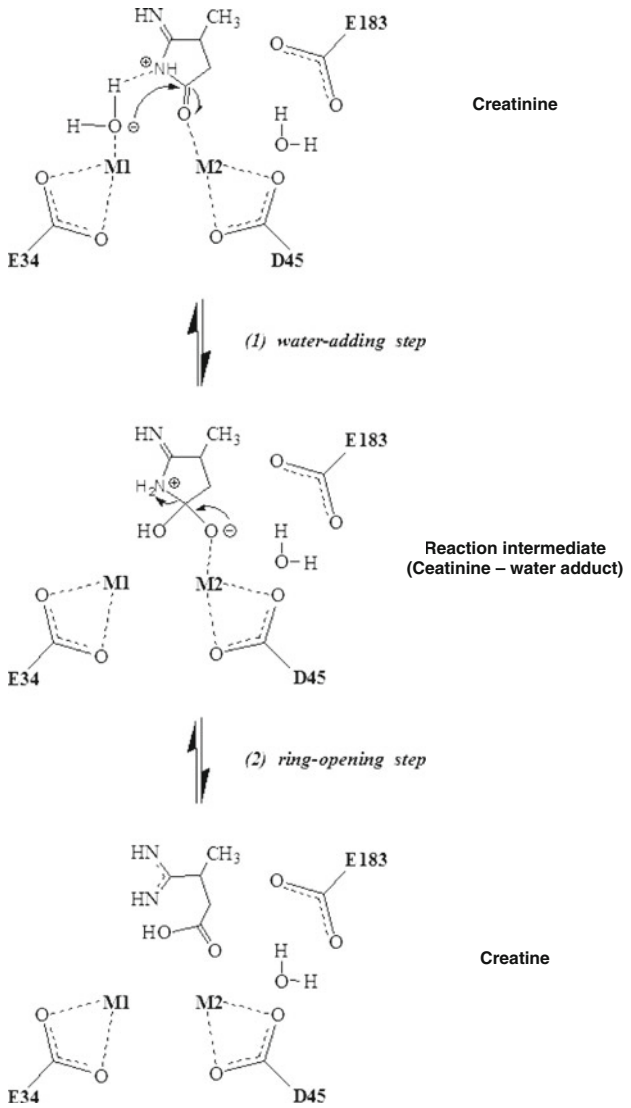


**Fig. 1** Reaction schemes for the bi-metal catalyzed reaction to convert creatinine to creatine. Scheme 1 (*top*): water adding step, scheme 2 (*bottom*): ring opening step

## Materials and methods

### 3D model building

The crystal structure of the creatininase complexes with the creatine product from *Peudomonas putida* has been solved in the protein data bank (PDB code: 1V7Z) at 1.8 Å resolution [7]. The enzyme is a typical $Zn^{2+}$ enzyme with a binuclear metal center ($Mn^{2+}$ and $Zn^{2+}$). The 3D X-ray crystallographic structure exhibited the binding site of the following amino acids, Glu34, His36, Val44, Asp45, Ser78, Gly79, His120, Tyr121, TRP154, ASP175, Glu177, His178 and Glu183, in 5.0 Å regions of the creatinine substrate. For $Mn^{2+}$-activated enzyme, $Mn^{2+}$ has a square-pyramidal geometry bound to three protein ligands of Glu34, Asp45, and His120 and two water molecules. $Zn^{2+}$ has a well-ordered tetrahedral geometry bound to the three protein ligands of His36, Asp45 and Glu183 and a water molecule as illustrated in Supplementary Fig. S1.

In order to clarify the nature of the substrate (creatinine) and product (creatine) species in the active site, the initial

structure creatininase-creatinine complex is modified from the X-ray structure of the creatininase-creatine complex. The creatinine as substrate was built from X-ray structure of creatine. Carbon and nitrogen bond was created to form the five membered ring. H1, H2, O6 was removed and the structure was minimized using conjugate gradient algorithm. Force field parameters for creatinine and creatine as in supplementary Table S1 for the creatinine according to AMBER atom type were modified using Gasteiger charge where no significant difference with HF/6-31G* RESP charges is observed as listed in Supplementary Table S2 Hydrogens were added to enzyme using the tLEaP program in AMBER 9.0 [10]. This program was also used to solvate the structure in a box of TIP3P water molecules within 10 Å from the enzyme-substrate complex.

## Molecular dynamic simulation

All molecular dynamics simulations were performed with the AMBER 9.0 program, together with the force field ff03 in the AMBER 9.0 package. The system was minimized and subjected to MD simulations. The water structures around complex were first optimized for 1,000 ps by slowly reducing force from 10.0, 5.0, 2.5 and 1.25 kcal $mol^{-1}$ $Å^{-2}$, respectively, while the enzyme and metals were fixed. The temperatures were gradually increased from 0 to 300 K in 60 ps, and kept constant at 300 K onwards. After the first 1,000 ps, only metal were fixed while the other parts were simulated without any constraint for another 1,000 ps. The time step of simulation was 2 fs with nonbonded cutoff of 12.0 Å. The particle mesh Ewald (PME) method was used to treat long-range electrostatic interactions, and bond lengths involving bonds to hydrogen atoms were constrained using SHAKE. This was conducted in order to relax the system and to remain the structure as close as possible to the initial X-ray structure. A total of 2 ns of MD were carried out and the last 500 ps snapshots were analyzed in details. Binding free energy decomposition was calculated using Molecular Mechanics Poisson-Boltzmann Surface Area (MM-PBSA) protocol from the trajectories collected with the *SANDER* program in AMBER 9.0. In this study, a total of 50 snapshots were taken at 10 ps time interval from the last 500 ps MD trajectories. The values of binding free energy ($\Delta G_{\text{binding}}$) were estimated from the absolute energy values in the gas phase ($E_{\text{gas}}$), the solvation free energies ($G_{\text{PB}} + G_{\text{nonpolar}}$), and the vibration, rotational, and translational entropies for the complex, creatininase, and creatinine. These terms were determined as previously reported [11, 12]. Here, we briefly describe the procedure:

$$\Delta G_{\text{bind}} = \Delta G_{\text{complex}} - \left[\Delta G_{\text{protein}} - \Delta G_{\text{ligand}}\right]$$

where the values of free energy for each species were evaluated by the following scheme:

$$\Delta G_{\text{water}} = E_{\text{MM}} + \Delta G_{\text{solvation}} - TS$$

$$G_{\text{solvation}} = G_{\text{solvation-electrostatic}} + G_{\text{nonpolar}}$$

$$E_{\text{MM}} = E_{\text{internal}} + E_{\text{electrostatic}} + E_{\text{vdw}}$$

$$E_{\text{internal}} = E_{\text{bond}} + E_{\text{angle}} - E_{\text{torsion}}$$

where the internal energy $E_{\text{internal}}$ has three contributions: $E_{\text{bond}}$, $E_{\text{angle}}$, and $E_{\text{torsion}}$, which represent the strain energy in bonds, angles and torsion angles caused by their deviation from the equilibrium values; $E_{\text{electrostatic}}$ and $E_{\text{vdw}}$ are the electrostatic and van der Waals interaction energy, respectively; $T$ is the temperature, $S$ is the entropy. $\Delta E_{\text{MM}}$ was calculated using the sander program in AMBER 9.0. $\Delta G_{\text{polar}}$ was computed by using the GB model whereas $\Delta G_{\text{non-polar}}$ was estimated based on the solvent-accessible surface area (SASA) as $\Delta G_{\text{non-polar}} = 0.0072 \times \text{SASA}$. The vdw radius of the $Mn^{2+}$ and $Zn^{2+}$ was set to 1.69 [13] and 1.10 Å [14], respectively.

## Transition state search

Two steps mechanism of water adding step and ring opening step as suggested in Fig. 1 were investigated with two systems of binuclear metal center, $Mn^{2+}/Zn^{2+}$ and $Zn^{2+}/Zn^{2+}$, of creatininase. Synchronous transit methods are used to find a transition state (TS) when the final MD structure of creatininase-creatinine, the optimized creatinine-water adduct, and the optimized X-ray structure of creatininase-creatine were used for initial, intermediate, and final configurations, respectively. Selected fragment in 3 Å regions from creatinine including Glu34, Asp45, Glu183, two waters and bi-metals with a total number atoms of 71 were subjected to transition search using Dmol3 module in Material Studio for the structure optimization and reaction path calculations [15–18]. All calculations were performed using density functional theory with local density approximation (LDA) of local functional PWC [19]. All electron core treatment with the DND basis set. Reaction paths were obtained using the linear synchronous transit (LST) and optimization calculation performs a single interpolation to a maximum energy, followed by the quadratic synchronous transit (QST) method for an energy maximum with constrained minimizations in order to refine the transition state to a high degree [20]. Another conjugate gradient minimization is performed on each point. The cycle is repeated until a stationary point is located or the number of allowed QST steps is exhausted. After the initial paths were converged, the highest energy points were optimized to the closest transition state (TS). Following the TS optimization the minimum energy path (MEP) between the critical points were calculated with the nudged elastic band (NEB) to

ensure continuity of the path and projection of the force so that the system converges to the MEP.

## Results and discussion

### Structural analysis of the creatininase-creatinine complex from MD simulations

From the last 500 ps MD simulations, root mean square fluctuations (RMSF) of amino acid residues were analyzed. The relative movement between the creatininase-creatinine complex and free creatininase due to different flexibility upon binding has been shown in Supplementary Fig. S2. High flexible loop for the complex, which is located outside the binding sites at amino acids, have been observed with the relative RMSF $> 0.5$ Å. The catalytic triad of MD structure as depicted in creatininase (supplementary Fig. S3, left) consisting of glutamine, aspartic and histidine, bi-nuclear metal and two water molecules are believed to be involved in the catalytic mechanism. In our study, water molecules are found to play an essential catalytic role and remains in the active site region during the MDs simulation which clarified by the distance of the O:WAT1 and O:WAT2 with creatinine at d5 $\sim$ 3.5 Å and d2 $\sim$ 5.0 Å, respectively, in Fig. 2. From the MD structure, water defined as WAT1 is more likely to act as proton donor to the NH position of the ring in the first step of the reaction. The fluctuations in the distance of water near $Mn^{2+}$ and $Zn^{2+}$ were determined from last 500 ps MDs simulations as shown in Fig. 2 and found to be stably confined in the binding pocket. The average distance was listed in Table 1. Most of distances remain relatively stable except the *d1* distance between the nitrogen of creatinine and hydrogen of WAT1, which varies between 2.5 and 4.5 Å. Binding

**Table 1** Average distance of water in binding with creatinine from last 500 ps of MD simulation

| Distance | Atom1 | Atom2 | Distance (Å) |
|---|---|---|---|
| d1 | WAT1:H2 | Creatinine:N3 | 3.058 |
| d2 | Creatinine:C1 | WAT2:O | 5.231 |
| d3 | Creatinine:O1 | $Mn^{2+}$ | 5.730 |
| d4 | Creatinine:O1 | $Zn^{2+}$ | 2.065 |
| d5 | Creatinine:N3 | WAT1:O | 2.921 |
| d6 | $Zn^{2+}$ | WAT2:O | 3.968 |
| d7 | $Mn^{2+}$ | WAT1:O | 2.326 |

residues within 5.0 Å from creatinine consists of Glu34, His36, Asp45, **Ser74,** His120, Tyr121, Glu122, Trp154, Trp174, Asp175, Glu177, His178 and Glu183 which are slightly different from those observed from the X-ray structure are Glu34, His36, Asp45, **Ser78, Gly79**, **Glu119,** His120, Tyr121, Glu122, Trp154, Trp174, Asp175, **Ile176,** Glu177, His178 and Glu183. The bold letters indicate the different. The binding pockets seem to be the hydrophilic-charged (Glu34, His36, Asp45, His120, Glu122, Asp175, Glu177, His178 and Glu183) pockets. For the investigation of hydrogen bonding with the distance <3.0 Å and angle 120°, several hydrogen bonds such as CRE:N2-WAT1:H2 and CRE:H1-WAT1:O, were found with 55.8 and 14.8% occupied, respectively. This observation indicated the role of water in forming hydrogen bonds with substrates.

### Decomposing energy of binding

Further insights into the catalytic mechanism of creatininase may be obtained by understanding the role of individual residues in catalysis. The binding free energy of the creatininase-creatinine complex was decomposed into contributions on per-residue basis using MM-GBSA

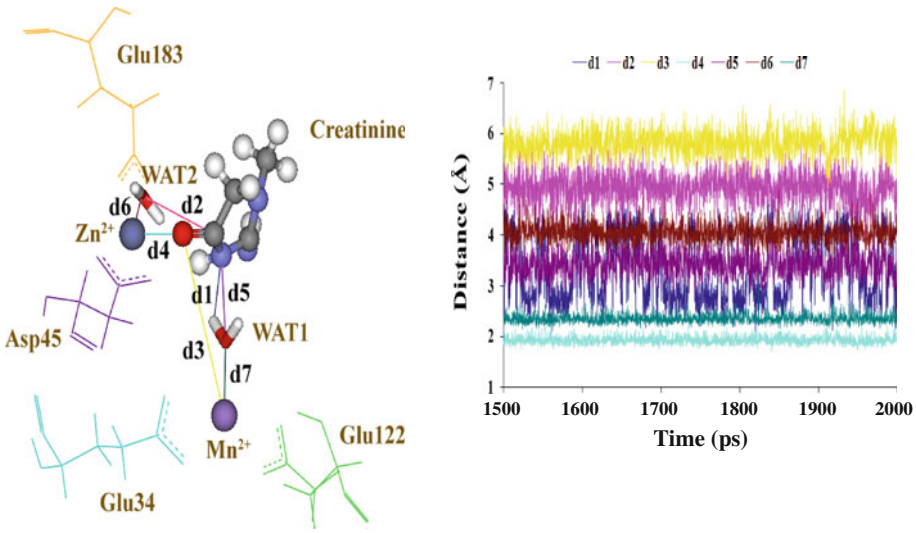


**Fig. 2** The time dependence of the distance involve in the reaction coordinate. The distances are depicted in the *left* figure

method. In this regard, an analysis of interaction energy of the amino acid residues with the creatinine can be decomposed into contributions per residue. A negative contribution denotes a stabilizing contribution whereas a positive one denotes a destabilizing contribution. The result was summarized in Table 2. The binding residues within 5.0 Å from creatinine that provide a significant contribution to stabilization with absolute total binding free energy (|TOT|) >0 kcal/mol are listed. As demonstrated, the creatinine substrate is highly favorable in binding as indicated by a large negative of TOT (−17.55 kcal/mol). Most amino acid residues listed in Table 2 and the plots in Supplementary Fig. S4 have similar amplitude of free energy which varies between −1 and −3 kcal/mol. The highly negative free energy is found in $Zn^{2+}$ (−7.48 kcal/mol) due to the electrostatic energy contribution. The three strong binding residues, Glu34, Asp45 and Glu183, which show higher negative free energy, may play a critical role in stabilization of $Zn^{2+}$ and these residues were selected for the transition state study. The unfavorable binding of $Mn^{2+}$ and His36 was observed as indicated by the positive free energy. For the high TOT energy in $Mn^{2+}$, it clearly showed in Table 2 that the ELE energy seems to be small (−9.6 kcal/mol) compared with that in $Zn^{2+}$ (∼−35.3 kcal/mol), which means that electrostatic interaction occur on Mn2+ is less favored than that occurs on $Zn^{2+}$. This could be that the $Mn^{2+}$ stays away from the surrounding charged residue, i.e., Glu34 or Glu122.

**Table 2** Decomposed energy of the binding residues in creatininase with creatinine

| Residue | VDW | ELE | GAS | GBSOL | TOT |
|---|---|---|---|---|---|
| Glu34 | −0.15 | 3.89 | 3.74 | −5.13 | −1.39 |
| His36 | 0.23 | 3.55 | 3.78 | −2.90 | 0.89 |
| Asp45 | 0.06 | 6.40 | 6.46 | −9.81 | −3.35 |
| Ser74 | −0.01 | −0.34 | −0.36 | 0.44 | 0.08 |
| His120 | −0.90 | −0.07 | −0.97 | 0.78 | −0.19 |
| Tyr121 | −1.07 | −0.42 | −1.50 | 0.31 | −1.19 |
| Glu122 | −0.18 | 3.46 | 3.28 | −3.65 | −0.36 |
| Trp154 | −0.99 | −0.42 | −1.41 | −0.10 | −1.51 |
| Trp174 | −0.84 | −1.12 | −1.96 | 0.67 | −1.29 |
| Asp175 | −0.67 | −2.25 | −2.92 | 1.60 | −1.33 |
| Glu177 | −1.40 | −0.70 | −2.10 | 0.33 | −1.76 |
| His178 | −1.08 | −1.69 | −2.77 | 2.13 | −0.65 |
| Glu183 | 0.43 | 6.70 | 7.13 | −9.57 | −2.44 |
| $Mn^{2+}$ | −0.02 | −9.63 | −9.65 | 12.66 | 3.01 |
| $Zn^{2+}$ | 1.65 | −35.31 | −33.66 | 26.18 | −7.48 |
| Creatinine | −7.28 | −26.91 | −34.19 | 16.63 | −17.55 |

VDW, ELE and GBSOL stands for Van der Waals energy, electrostatic energy and generalized Born model solvation free energy in kcal/mol, respectively; GAS = VDW + ELE, and TOT = GAS + GBSOL

A slightly positive MM-PBSA total energy with His36 may be due to the close distance between the HN atom of His36 and $Zn^{2+}$, as seen in Fig. S1, causing a higher positively ELE energy (∼3.5 kcal/mol) compared to that in His120 (∼−0.1) and His178 (∼−1.7). This seems to depend on the solvation term (GBSOL) as well since this term is higher negative compared with the positive values in other histidines (see His120, His178 in Table 2). Overall Van der Waal (Vdw) interaction is not different. Most of the differences in interaction observed are electrostatic. Additionally, all residues in Table 2 may play an important role to substrate binding.

## Reaction mechanism

In this subsection we illustrate the results relating to the reaction mechanisms. Referring to a previously proposed mechanism by Yoshimoto et al. [7] that two water molecules are remained in the active site region and found to play an essential catalytic role.; therefore, we aimed to explore the reaction pathways. From the position of water in MD simulation, WAT1 shows its role in the catalytic mechanism observed from the dynamics distances of *d1* (3.5–4.0 Å) between H: WAT1 and creatinine while WAT2 is rather stable as also proposed in Fig. 1. From the position of water in MD simulation, the more probable pathway is through $Mn^{2+}$ catalyzed reaction via WAT1. We have used linear synchronous transit (LST) method and the quadratic synchronous transit (QST) to find the transition state. The LST method generates an estimate of the transition state by finding the highest point along shortest line connecting two minima. The QST method extends this further by subsequently searching for a minimum along a line perpendicular to the previous one. The path connecting minima and the found point were searched for a saddle point. Minimum energy pathway (MEP) along the potential energy surface (PES) was identified. One imaginary frequency was found for the transition states. QM systems of MD and X-ray structure in supplementary Fig. S3 were modified, which the $Mn^{2+}$ was changed to $Zn^{2+}$. The creatinine-water adduct intermediate was obtained when hydrogen (H) from water attached to nitrogen (N) from creatinine and hydroxyl of water attached to the ring carbon at carbonyl group (C=O). This intermediate is stabilized by a partial ionic bond between the $Mn^{2+}$/$Zn^{2+}$ ion and the negative charge on the oxygen. The profile of energy changes of the two pathways, $Mn^{2+}$/$Zn^{2+}$ and $Zn^{2+}$/$Zn^{2+}$ with LDA/PWC levels of theory are shown in Fig. 3. It can be seen that the activation energy (Ea) of the first step reaction for pathway of $Mn^{2+}$/$Zn^{2+}$ is higher than pathway of $Zn^{2+}$/$Zn^{2+}$ with the energy of 8.84 kcal/mol. This is due to the charge delocalization in TS which $Zn^{2+}$ stabilizes more than $Mn^{2+}$ and causes a decrease in Ea

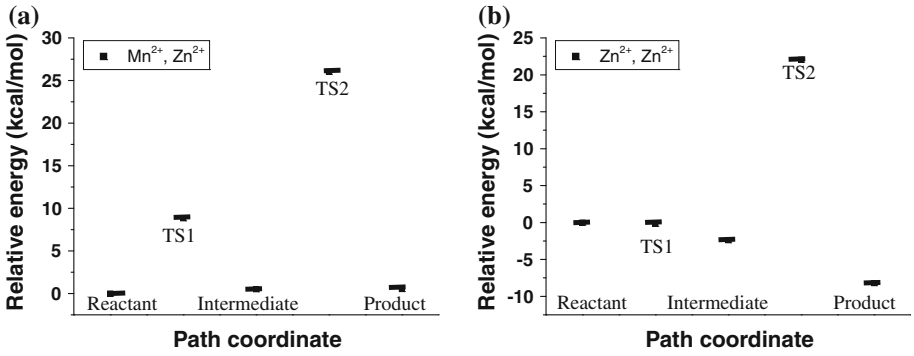


**Fig. 3** Calculated reaction paths for the manganese (**a**) and zinc (**b**) catalyzed reactions from X-ray structure (PDB code = 1V7Z)

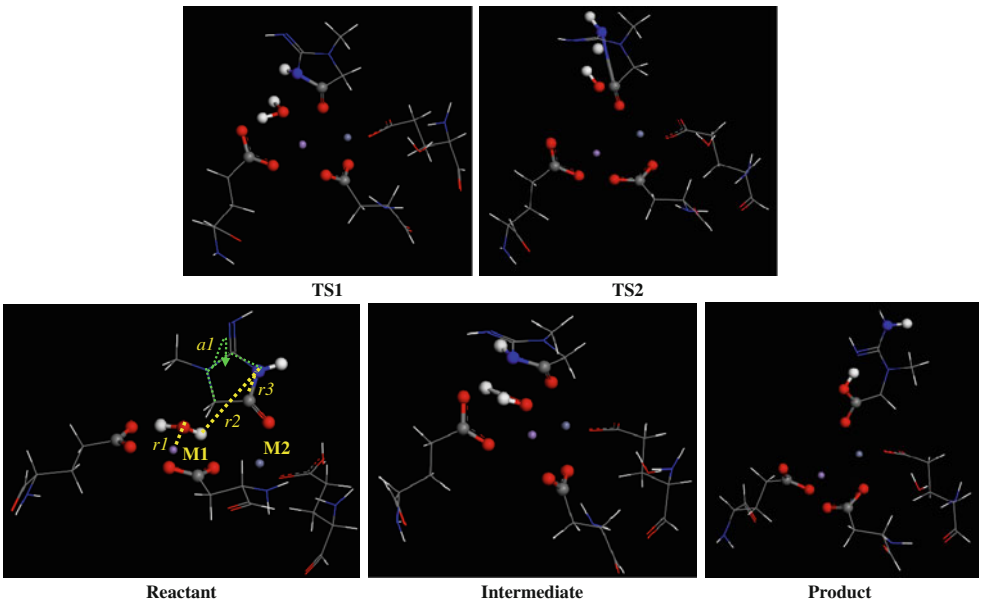


**Fig. 4** The structure of the reactant, transition states, intermediate and the product involved in the reaction mechanism

which in turn increases the rate of reaction as expected. The second step of the two pathways yields the similar energy barrier of 26.03 and 24.44 kcal/mol for $Mn^{2+}/Zn^{2+}$ and $Zn^{2+}/Zn^{2+}$, respectively. The exothermic process was found in the latter system with the energy of products, which is lower than that of the reactant by approximately 8.98 kcal/mol. This observation also indicated that the rate determining step is the second step. Therefore, according to the obtained results, the mechanism is basically consistent with the mechanism proposed by Yoshimoto et al. and the reaction in converting creatinine to creatine occurs in a preferable pathway involving with $Zn^{2+}/Zn^{2+}$. Distances, torsion angle parameters, and electrostatic charges of the structures, as illustrated in Fig. 4 corresponding to reactant, transition state, intermediate and product, are reported in Table 3. It is apparent that *r2* decreases in TS1 respect to reactant due to the mechanism involving in attachment of water to NH of substrate. On the contrary, *r3* increases due to the ring opening to form the creatine with the torsion angle change from 1.9° found in reactant to −159.1 degree in product. Possible mechanism over the barrier catalysis is found to be the stabilization of charged transition states by residues in the active site forming ionic bonds (or partial ionic charge interactions) with the intermediate. Charge distribution in the reactants and TS particularly shows a large change in charges of N1, C3, O5, and C2, O3, O4 of Asp45 and transition metal cofactors, zinc or manganese.

## Conclusion

Our simulations have elucidated the two steps mechanism, water adding step and ring opening step, in converting the creatinine to creatine by which two metal ions and water molecules coadjuvate the creatininase. A complete understanding of the functional role of different metal ion cofactors with the calculated energy barriers can be obtained by investigating the active site in the region of the transition state using a combined *ab initio* quantum mechanical/molecular mechanical (QM/MM) approach and

**Table 3** Selected distances and electric charge variations for reactant, TS, intermediate and product

| Distance (Å) | M1 = $Mn^{2+}$/M2 = $Zn^{2+}$ system | | | | | M1 = $Zn^{2+}$/M1 = $Zn^{2+}$ system | | | | |
|---|---|---|---|---|---|---|---|---|---|---|
| | *R* | TS1 | *I* | TS2 | *P* | *R* | TS1 | *I* | TS2 | *P* |
| *r1* O:WAT1–Zn12 +) | 1.96 | 2.04 | 1.99 | 1.88 | 6.25 | 2.04 | 2.04 | 2.05 | 1.88 | 6.04 |
| *r2* (H:WAT1–N:substrate) | 5.76 | 4.50 | 2.74 | 1.04 | 1.04 | 5.10 | 4.50 | 2.94 | 1.04 | 1.04 |
| *r3* (N:Substrate–C:Substrate) | 1.37 | 1.37 | 1.37 | 3.49 | 4.53 | 1.37 | 1.37 | 1.37 | 3.49 | 4.53 |
| *a1*(N–C–N–C) | 1.90 | −2.80 | −7.90 | −51.70 | −159.10 | 1.50 | −2.80 | −7.40 | −51.70 | −159.00 |
| Atom | Charges for $Zn^{2+}$/$Zn^{2+}$ system | | | | | Charges for $Zn^{2+}$/$Zn^{2+}$ system | | | | |
| | *R* | TS1 | *I* | TS2 | *P* | *R* | TS1 | *I* | TS2 | *P* |
| Glu34:C1 | 0.490 | 0.623 | 0.449 | 0.470 | 0.465 | 0.578 | 0.655 | 0.440 | 0.525 | 0.418 |
| Glu34:O1 | −0.500 | −0.538 | −0.535 | −0.481 | −0.543 | −0.516 | −0.541 | −0.526 | −0.482 | −0.450 |
| Glu34:O2 | −0.606 | −0.585 | −0.519 | −0.552 | −0.520 | −0.634 | −0.555 | −0.490 | −0.538 | −0.464 |
| Asp45:C2 | 0.512 | 0.223 | 0.206 | 0.411 | 0.141 | 0.623 | 0.248 | 0.216 | 0.397 | 0.270 |
| Asp45:O3 | −0.491 | −0.381 | −0.492 | −0.378 | −0.289 | −0.830 | −0.349 | −0.357 | −0.346 | −0.257 |
| Asp45:O4 | −0.774 | −0.274 | −0.386 | −0.496 | −0.234 | −0.388 | −0.271 | −0.398 | −0.488 | −0.250 |
| WAT1:O6 | −0.835 | −0.856 | −0.939 | −0.561 | −0.475 | −0.739 | −0.828 | −0.648 | −0.528 | −0.458 |
| WAT1:H1 | 0.362 | 0.372 | 0.389 | 0.423 | 0.399 | 0.416 | 0.366 | 0.427 | 0.379 | 0.381 |
| WAT1:H2 | 0.503 | 0.541 | 0.552 | 0.330 | 0.338 | 0.379 | 0.532 | 0.341 | 0.329 | 0.339 |
| Substrate:N1 | −0.390 | −0.169 | −0.196 | −0.646 | −0.728 | −0.318 | −0.158 | −0.169 | −0.638 | −0.710 |
| Substrate:C3 | 0.524 | −0.047 | −0.056 | −0.416 | 0.863 | 0.407 | −0.033 | −0.115 | −0.400 | 0.855 |
| Substrate:O5 | −0.600 | −0.301 | −0.282 | −0.151 | −0.606 | −0.577 | −0.298 | −0.282 | −0.153 | −0.636 |
| Substrate:H3 | 0.300 | 0.267 | 0.290 | 0.318 | 0.356 | 0.292 | 0.265 | 0.265 | 0.320 | 0.353 |
| $M1^{2+}$ | 1.007 | 0.707 | 0.816 | 0.749 | 0.653 | 1.269 | 0.627 | 0.623 | 0.661 | 0.522 |
| $M2^{2+}$ | 1.185 | 0.563 | 0.609 | 0.592 | 0.570 | 0.765 | 0.562 | 0.589 | 0.617 | 0.589 |

classical molecular dynamics (MD) simulations. The transition states for these reactions were investigated using density functional theory (DFT) in combination with the linear (LST) and quadratic synchronous transit (QST) methods. The large discrepancy of the two different metal ion systems, $Mn^{2+}$/$Zn^{2+}$ as resolved from crystal structure and $Zn^{2+}$/$Zn^{2+}$ as our proposed, was found in the values of the lower energy barrier ( ~ 9 kcal/mol) of the latter system for the water adding step. The calculated barrier of both systems in the second step for ring opening was not much different. These findings have confirmed earlier suggestions that a crucial role in the reaction is played by water molecules and metal ions. A new perspective has shed the light in understanding the role of metal ions in biological processes.

**Acknowledgments** The authors would like to express grateful acknowledgement to the Thailand Research Fund (TRF), Computational Nanoscience Consortium (CNC), and National Nanotechnology Center (NANOTEC Thailand) for the access to Discovery Studio Version 1.7 program package. The authors also acknowledge a financial support from the Center for Innovation in Chemistry (PERCH-CIC), and Commission on Higher Education, Ministry of Education of Thailand.

## References

1. Spencer K (1986) Analytical reviews in clinical biochemistry: the estimation of creatinine. Ann Clin Biochem 23:1–25
2. Narayana S, Appleton HD (1986) Creatinine: a review. Clin Chem 26:1119–1126
3. Tietz NW (1986) Textbook of clinical chemistry. Saunders, Philadelphia, pp 1810–1857
4. Sena SF, Syed D, McComb RB (1988) Effect of high creatine content on the Kodak single-slide method for creatinine. Clin Chem 34:594–595
5. Pandey PC, Mishra AP (2004) Novel potentiometric sensing of creatinine. Sensor Actuator B Chem 99:230–235
6. Premanode B, Toumazou C (2007) A novel, low power biosensor for real time monitoring of creatinine and urea in peritoneal dialysis. Sensor Actuator B Chem 120:732–735
7. Yoshimoto T, Tanaka N, Kanada N, Inoue T, Nakajima Y, Haratake M, Nakamura KT, Xu Y, Ito K (2004) Crystal structures of creatininase reveal the substrate binding site and provide an insight into the catalytic mechanism. J Mol Biol 337:399–416
8. Tanaka N, Kusakabe Y, Ito K, Yoshimoto T, Nakamura KT (2002) Crystal structure of formaldehyde dehydrogenase from *Pseudomonas putida*: the structural origin of the tightly bound cofactor in nicotinoprotein dehydrogenases. J Mol Biol 324:519–533
9. Ito K, Kanada N, Inoue T, Furukawa K, Yamashita K, Tanaka N, Nakamura KT, Nishiya Y, Sogabe A, Yoshimoto T (2002) Preliminary crystallographic studies of the creatinine

amidohydrolase from *Pseudomonas putida*. Acta Crystallogr D 58:2180–2181
10. Case DA, Cheatham Iii TE, Darden T, Gohlke H, Luo R, Merz KM Jr, Onufriev A, Simmerling C, Wang B, Woods RJ (2005) The Amber biomolecular simulation programs. J Comput Chem 26:1668–1688
11. Massova I, Kollman PA (2000) Combined molecular mechanical and continuum solvent approach (MM- PBSA/GBSA) to predict ligand binding, Perspect. Drug Discov Des 18:113–135
12. Wang JM, Hou T, Xu X (2006) Recent advances in free energy calculations with a combination of molecular mechanics and continuum models. Curr Comput Aided Drug Des 2:287–306
13. Bradbrook GM, Gleichmann T, Harrop SJ, Habash J, Raftery J, Kalb J, Yariv J, Hillier IH, Helliwell JR (1998) X-ray and molecular dynamics studies of concanavalin-A glucoside and mannoside complexes: Relating structure to thermodynamics of binding. J Chem Soc Faraday Trans 94:1603–1611
14. Merz KM Jr (1991) $CO_2$ binding to human carbonic anhydrase II. J Am Chem Soc 113:406–411
15. Frisch MJ, Trucks GW, Schlegel HB, Scuseria GE, Robb MA, Cheeseman JR, Zakrzewski VG, Montgomery JA, Stratmann RE, Burant JC, Dapprich S, Millam JM, Daniels AD, Kudin KN, Strain MC, Farkas O, Tomasi J, Barone V, Cossi M, Cammi R, Menucci B, Pomelli C, Adamo C, Clifford S, Ochterski J, Petersson GA, Ayala PY, Cui Q, Morokuma K, Malick DK, Rabuck AD, Raghavachari K, Foresman JB, Cioslowki J, Ortiz JV, Stefanov BB, Liu A, Liashenko A, Piskorz P, Komaromi I, Gomperts R, Martin RL, Fox DJ, Keith T, Al-Laham MA, Peng CY, Nanayakkara A, Gonzalez M, Callacombe M, Gill PMW, Johnson BG, Chen W, Wong MW, Andres JL, Head-Gordon M, Replogle ES, Pople JA, Gaussian03 Program (1998)
16. Accelrys Software Inc (2007) Materials modeling and simulation software, release 4.3. Accelrys Software Inc, San Diego
17. Delley BJ (1990) DMOL is available commercially from BIO-SYM technologies, San Diego, CA. Chem Phys 92:508
18. Delley BJ (2000) Dmol3 is available as part of materials studio. Chem Phys 113:7756
19. Perdew JP, Wang Y (1992) Accurate and simple analytic representation of the electron-gas correlation energy. Phys Rev B 45:13244–13249
20. Halgren TA, Lipscomb WN (1977) The synchronous-transit method for determining reaction pathways and locating molecular transition states. Chem Phys Lett 49:225–232